ACS APPLIED MATERIALS & INTERFACES

Research Article

www.acsami.org

Fast Response and High Sensitivity Europium Metal Organic Framework Fluorescent Probe with Chelating Terpyridine Sites for Fe^{3+}

Min Zheng,[†] Huaqiao Tan,[†] Zhigang Xie,*[,‡] Ligong Zhang,[†] Xiabin Jing,[‡] and Zaicheng Sun*[,†]

[†]State Key Laboratory of Luminescence and Applications, Changchun Institute of Optics, Fine Mechanics, and Physics, Chinese Academy of Sciences, 3888 East Nanhu Road, Changchun, Jilin 130033, P.R. China.

[‡]State Key Laboratory of Polymer Physics and Chemistry, Changchun Institute of Applied Chemistry, Chinese Academy of Sciences, 5625 Renmin Street, Changchun, Jilin 130022, P.R. China.

Supporting Information

ABSTRACT: Iron is one of the most important elements in the metabolic process for all living system. However, both its deficiency and excess from normal permissible limits can induce serious disorders. We synthesized a europium-based metal−organic framework (Eu-MOF), $\mathbf{EuL_3}$ (**L** = 4′-(4-carboxyphenyl)-2,2′: 6′,2″-terpyridine), under hydrothermal conditions, and used it as a solid luminescence sensor for Fe^{3+} ions. The robust $\mathbf{EuL_3}$ shows fast response (∼ 1 min) and high sensitivity (Stern−Volmer constant $K_{SV} = 4.1 \times 10^3$ L/mol) for Fe^{3+} ions in aqueous solution or biological systems due to the existence of chelating terpyridine and open channels. The simple and portable test paper based on the EuL_3 fluorescent sensor system provides a convenient and reliable detection of Fe^{3+} in every day applications. This pioneering work contributes to extend the potential application of Ln-MOFs to the biological and environmental areas.

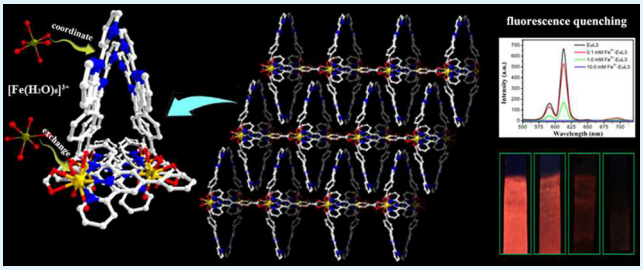

KEYWORDS: *terpyridine, europium metal organic framework, fluorescent probe, Fe^{3+} ion, Fe^{3+} test paper, open channel*

INTRODUCTION

Iron is a ubiquitous metal in cells and plays a crucial role in a variety of vital cell functions such as oxygen metabolism and electron transfer processes in DNA and RNA synthesis.[1] However, both excess and deficiency from the normal permissible limit can induce serious disorders. A deficiency of iron limits oxygen delivery to cells, resulting in fatigue, poor work performance, and decreased immunity.[2] Conversely, excess amounts of iron ions in a living cell can catalyze the production of reactive oxygen species (ROS) via the Fenton reaction, which can damage lipids, nucleic acids, and proteins.[3] The cellular toxicity of iron ions has been connected with serious diseases, including Alzheimer's, Huntington's, and Parkinson's disease.

The considerable importance of iron in biological and environmental systems has led to increasing interest in recent years in the development of selective techniques for determination of iron. Various analytical techniques such as spectrophotometry,[4] inductively coupled plasma mass spectrometry,[5] voltammetry,[6] and atomic absorption spectroscopy[7] have been developed for sensitive iron determination, but several other metal ions were shown to interfere, necessitating complicated pretreatment procedures and sophisticated instrumentation. Recently, fluorescent sensors have been widely investigated for selective detection of iron because of their ability to provide a simple, sensitive, selective, precise, and economical method for online monitoring without any pretreatment of the sample together with the advantages of spatial and temporal resolution.[8]

Lanthanides (Lns) are fascinating due to their versatile coordination geometry, unique luminescent and magnetic properties, and high framework stability.[9−11] Particularly, the brilliant optical properties of Ln-MOFs make them attractive for potential applications such as fluorescent probes and luminescent bioassays.[12−17] In fact, some Ln-MOFs have been successfully employed for the sensing of small molecules (for instance TNT[12] and acetone[14]) and ions (such as Zn^{2+}, Cu^{2+}, Mg^{2+}, Ag^{+}, F^{-}, etc.).[18−21] However, little work has been devoted to the development of fluorescent probes that are sensitive to Fe^{3+} ions.[22,23] Very recently, Dang et al. showed the first example of Eu-MOF fluorescent sensor for Fe^{3+}.[24] However, the detective sensitivity was limited by its fluorescent quenching caused by cation exchange.

In designing highly sensitive and selective fluorosensors, the chelating agent (receptor unit) should have the potential to interact with the target metal ion (analyte) selectively and efficiently, and also the chelating unit must be connected to a suitable fluorophore unit that produces a distinct fluorescence

Received: November 27, 2012
Accepted: January 18, 2013
Published: January 18, 2013

upon chelation. Once the analyte is recognized by the receptor, the fluorescence signals can be observed in the form of quenching or enhancement in the fluorescence maxima due to either electron transfer (ET), charge transfer (CT), or energy transfer (ET) processes.[25,26] Herein, we present a luminescent MOF material **EuL$_3$** (HL = 4′-(4-carboxyphenyl)- 2,2′: 6′,2″-terpyridine, see Figure 1a), as a fast response and high sensitivity solid fluorescent probe targeted for Fe^{3+} ions due to its dual functional ligand group. Owing to the preferential binding of lanthanide ions to carboxylate oxygen atoms over the pyridyl nitrogen atom in Ln^{3+}-pyridinecarboxylate complexes,[19,27] free terpyridine groups are left as a high efficient receptor unit ready for detecting cations. At the same time, Eu^{3+} ion, as a luminescence center, is linked with the receptor unit through a phenylcarboxylic acid. Once Fe^{3+} ions bind with the terpyridine group, the luminescence of the fluorophore unit (Eu^{3+}) is quenched rapidly. That results in very short response time (~1 min) of ground EuL_3 microcrystals on paper. The Stern−Volmer constant of EuL_3 in Fe^{3+} aqueous solution reaches 4.1×10^3 L/mol, which is the best value for the solid Ln-MOF fluorescent probe to our knowledge.

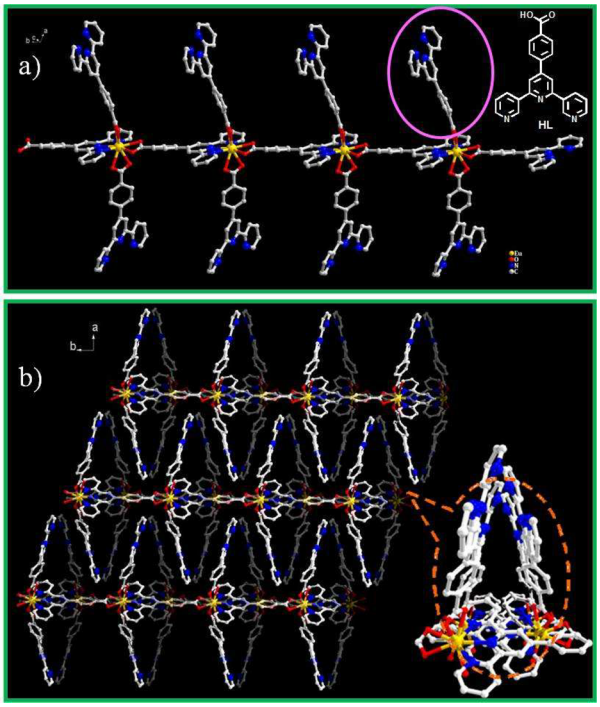

Figure 1. Perspective view of the 1D chain (a) and AB layer along the *c* axis (b) in **EuL$_3$**. All H atoms are omitted for clarity.

EXPERIMENTAL SECTION

Typical Synthesis of HL and EuL$_3$. All reagents were purchased commercially and used without further purification. HL was synthesized according to the literature method with some modification.[28] **EuL$_3$** was prepared by hydrothermal reaction of $Eu(NO_3)_3{\cdot}6H_2O$ (0.10 mmol), **L** (0.10 mmol), and NaOH (0.10 mmol) in 10 mL of deionized water at 160 °C for 24 h. After cooling to room temperature, crystals were collected by filtration with yield of 30% based on $Eu(NO_3)_3{\cdot}6H_2O$.

Luminescence Quenching Experiments. **EuL$_3$** crystals were simply immersed in the aqueous solutions of $M(NO_3)_x$ at room temperature (M = Na^+, K^+, Mg^{2+}, Ca^{2+}, Ba^{2+}, Fe^{2+}, Ni^{2+}, Al^{3+}, Cr^{3+}, Pb^{2+}, Cd^{2+}, Cu^{2+}, Zn^{2+}, Ag^+, Co^{2+}, Fe^{3+}, respectively) to form metal-EuL_3 compounds (M^{n+}-EuL_3).

Paper Based Fluorescent Sensor. The filter paper was cut into strips of 1 cm × 2.5 cm. The strips were dipped in the dispersion of EuL_3 in ethanol for 1 min, and then taken out and left to dry at room temperature. The EuL_3 strips were immersed into aqueous $Fe(NO_3)_3$ solution of different concentrations for 1 min.

Characterization. Thermogravimetric analysis (TGA) was made using a SDT 2960 Simultaneous DSC-TGA of TA Instruments up to 800 °C, and the heating rate was 10 °C min^{-1} under an air flow of 100 mL min^{-1}. X-ray power diffraction (XRD) was performed on a D8 Focus (Bruker) diffractometer with Cu 40 Kα radiation field-emission (λ = 0.15405 nm, continuous, 40 kV, 40 mA, increment = 0.02°). Suitable crystals with dimensions of 0.29 × 0.28 × 0.10 mm^3 were selected for single crystal X-ray diffraction analysis. Crystallographic data were collected at 273 K on a Bruker Apex II CCD diffractometer with graphite monochromated Mo Kα radiation (λ = 0.71073 Å). Data processing was accomplished with the SAINT program. The structure was solved by direct methods and refined on F^2 by full-matrix least-squares using SHELXTL-97. Non-hydrogen atoms were refined with anisotropic displacement parameters during the final cycles. All hydrogen atoms of the organic molecule were placed by geometrical considerations and were added to the structure factor calculation. Isolated solvents within the channels were not crystallographically well-defined. The luminescence spectra were recorded on a Hitachi F-4500 fluorescence spectrophotometer. The photomultiplier tube (PMT) voltage was 700 V, the scan speed was 240 nm·min^{-1}, and the slit width of excitation and emission is 2.5 nm. The strongest emission wavelengths were located at 612 nm when excitation was at 350 nm.

RESULTS AND DISCUSSION

EuL$_3$ was prepared by hydrothermal reaction of $Eu(NO_3)_3{\cdot}6H_2O$ (0.01 mol), HL (0.01 mol) and NaOH (0.0001 mol) in 10 mL of deionized water at 160 °C for 24 h.[25] The reaction products were single crystals of microscale with a chemical composition of $C_{66}H_{42}EuN_9O_6$ as determined by single-crystal X-ray diffraction (See Table S1 in Supporting Information). Thermogravimetric analysis (Supporting Information Figure S1a) results indicate that there is no solvent molecule (water) in the MOF structure, because **L** is bulky and multidentate, and thus can prevent the lanthanide ions from coordinating with solvent molecules and anions. The phase purity of the bulk material was independently confirmed by powder X-ray diffraction (XRD, red line in Figure 6). The X-ray structure analysis reveals a 1D framework of **EuL$_3$** (Figure 1a), in agreement with the Hu group's report.[29] Each Eu^{3+} ion is nine-coordinated by six oxygen atoms from three **L**-anions and three nitrogen atoms from one **L**-anion with distorted tricapped trigonal prism geometry. In this compound, **L**-anions coordinate to Eu^{3+} ions in two different coordination fashions and play different roles in the formation of the frameworks (Figure 1a): (1) on the backbone, **L**-anions adopt pentadentate coordination fashion in which the carboxylate group adopts the bidentate chelating coordination mode and the terpyridyl moiety acts as the tridentate-chelating coordination mode with two terminal pyridyl rings in a *cis* arrangement, forming a 1D infinite chain running along the *a* axis; (2) on the arms, the carboxylate group adopts a bidentate chelating coordination mode and the terpyridyl moiety is free with two terminal pyridyl rings in a *trans* arrangement. These free Lewis basic terpyridyl sites are expected to accept small Lewis acidic molecules or metal ions. Moreover, the neighboring chains pack together through the $\pi\cdots\pi$ stacking interactions and C−H$\cdots\pi$ interactions to form a 3D supramolecular structure. It is

dx.doi.org/10.1021/am302862k | ACS Appl. Mater. Interfaces 2013, 5, 1078−1083

worth noting that the channels formed between the layers (Figure 1b) are very helpful to cation transportation.

The luminescence spectra of **EuL$_3$** are shown in Figure 2. The excitation peak around 250 nm is ascribed to the

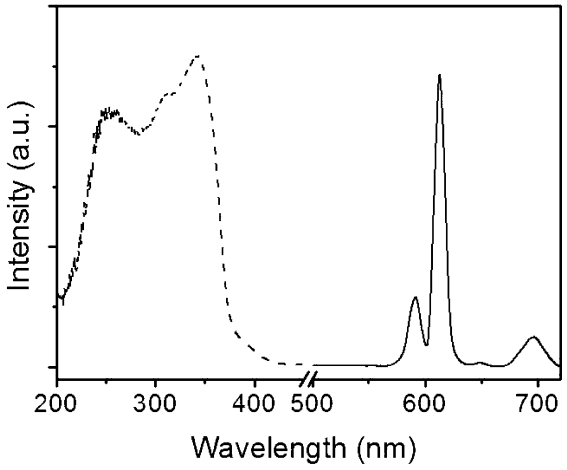

Figure 2. Excitation (dashed, λ_{em} = 612 nm) and emission spectra (solid, λ_{ex} = 350 nm) of **EuL$_3$**, solid samples.

absorption of **L** ligands, and those at 313 and 342 nm are from the absorption of the Eu^{3+} ion. The emission spectra of **EuL$_3$** excited at 350 nm reveals well-resolved magnified luminescence of the f−f transitions, attributed to the energy transfer from **L** ligands to Eu^{3+} ions. Characteristic transitions of the Eu^{3+} ion are also evident with peaks at 592, 612, 649, and 696 nm, which could be attributed to $^5D_0 \rightarrow {}^7F_1$, $^5D_0 \rightarrow {}^7F_2$, $^5D_0 \rightarrow {}^7F_3$, and $^5D_0 \rightarrow {}^7F_4$ transitions, respectively.

EuL$_3$ was simply immersed in an aqueous solution of 0.01 mol/L $M(NO_3)_x$ (M = Na^+, K^+, Mg^{2+}, Ca^{2+}, Ba^{2+}, Fe^{2+}, Ni^{2+}, Al^{3+}, Cr^{3+}, Pb^{2+}, Cd^{2+}, Cu^{2+}, Zn^{2+}, Ag^+, Co^{2+}, Fe^{3+}, respectively) for 20 h to form metal-ion-incorporated M^{n+}-**EuL$_3$** as solids for luminescence studies. The photoluminescence properties of M^{n+}-**EuL$_3$** are recorded and compared in Figure 3. Characteristic emissions of the Eu^{3+} ion are evident for most of M^{n+}-**EuL$_3$** except in the case of the Fe^{3+} ion. Most interestingly, the luminescence intensity of M^{n+}-**EuL$_3$** heavily depends on the type of metal ion: alkaline metal ion such as K^+ and alkaline-earth metal ions have basically no effect on the Eu-luminescence, while transition metal cations have varying

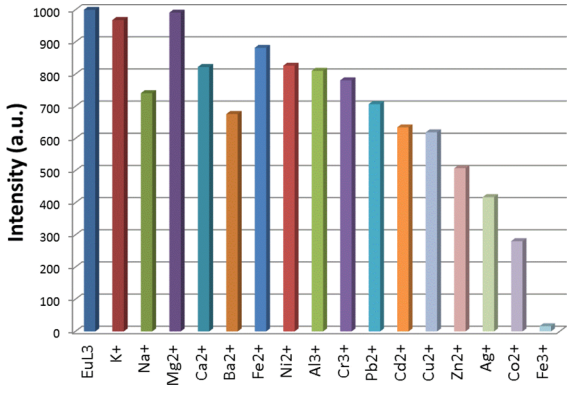

Figure 3. Photoluminescence intensity of the $^5D_0 \rightarrow {}^7F_2$ transition (612 nm) of **EuL$_3$** treated with 0.01 mol/L different metal ions for 20 h, excited at 350 nm.

degrees of quenching effects on the luminescence intensity. The luminescence intensity at 612 nm is about half of the original one after immersing into 0.01 mol/L Zn^{2+}, Ag^+, and Co^{2+} aqueous solution for 20 h. Impressively, there is almost no characteristic emission of Eu^{3+} ions for Fe^{3+}-**EuL$_3$** within a very short period. The main reason is that binding of Fe^{3+} to the free terpyridyl nitrogen atoms results in fluorescence quenching of **EuL$_3$** crystals. Probably, the paramagnetic effect caused by the unpaired d-electrons present in Fe^{3+} promotes dissipation of the excited state energy in a nonradiative process. Compared with other metal cations, **EuL$_3$** shows a high selectivity to Fe^{3+} ion.[26]

The quenching effect of **EuL$_3$** was examined as a function of $Fe(NO_3)_3$ concentration in the range of 0−0.05 mol/L. The **EuL$_3$** solid samples were immersed in different concentrations of $Fe(NO_3)_3$ for 24 h, and then their luminescence intensity at 612 nm was recorded. As shown in Figure 4, the fluorescence

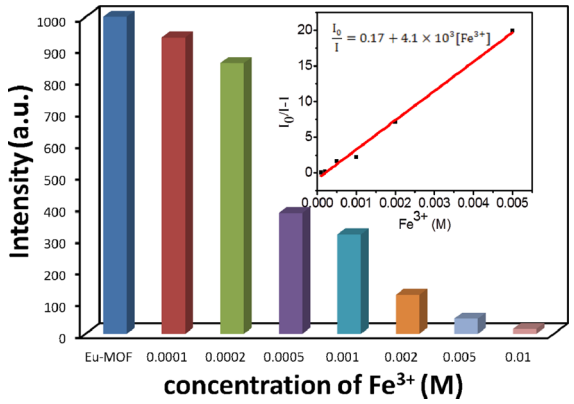

Figure 4. Fluorescence intensity of Fe^{3+}-**EuL$_3$** solid sample at 612 nm as a function of $Fe(NO_3)_3$ concentration in solution, λ_{ex} = 350 nm. The insert is Stern−Volmer plot of **EuL$_3$** quenched by $Fe(NO_3)_3$ aqueous solution.

intensity vs $[Fe^{3+}]$ plot can be curve-fitted into $(I_0/I) - 1 = K_{SV}[Fe^{3+}] - 0.83$, close to the Stern−Volmer equation:

$$(I_0/I) - 1 = K_{SV}[M]$$

where I_0 and I are the luminescent intensity before and after metal ion incorporation, respectively; [M] is the metal ion molar concentration; and K_{SV} is the Stern−Volmer constant. On the basis of the experimental data in Figure 4, the K_{SV} value is calculated to be 4.1 × 10^3 L/mol. This K_{SV} value is comparable to those in well-designed solution base organic compounds for sensing of Fe^{3+} (typical K_{SV} of about 10^4 L/mol).[26]

The existence of channels and chelating terpyridine groups in the **EuL$_3$** MOF provides an opportunity for fast response to the analyte Fe^{3+}. To confirm this hypothesis, the fluorescence intensity of **EuL$_3$** at 612 nm (λ_{ex} = 350 nm) was measured as a function of immersion time in aqueous solution of 0.01 mol/L. As shown in Figure 5, more than half of the PL intensity of pure **EuL$_3$** was decreased when **EuL$_3$** was treated with Fe^{3+} solution for 10 min. This response is much faster than that in the previous report (about 24 h).[22] The main reason is that Fe^{3+} ions can rapidly diffuse into the channels of **EuL$_3$** crystals and bind to the free terpyridine groups, and the interaction between Fe^{3+} and **L** reduces the energy transfer efficiency from **L** to the Eu^{3+} ion, resulting in immediate photoluminescence quenching. With more and more Fe^{3+} ions binding to free

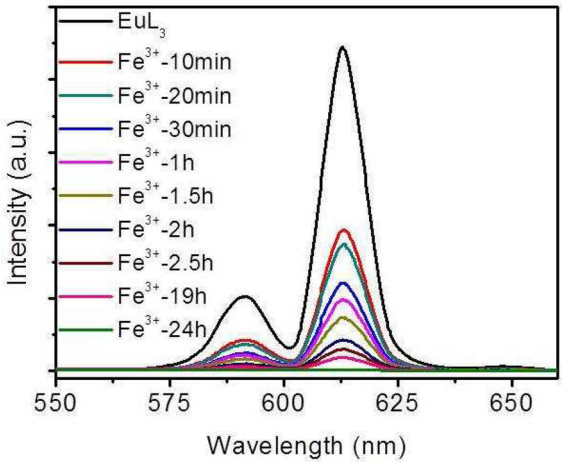

Figure 5. Variation of fluorescence intensity of Fe^{3+}-**EuL_3** solid sample at 612 nm with immersion time in $Fe(NO_3)_3$ solution of 0.01 mol/L, λ_{ex} = 350 nm.

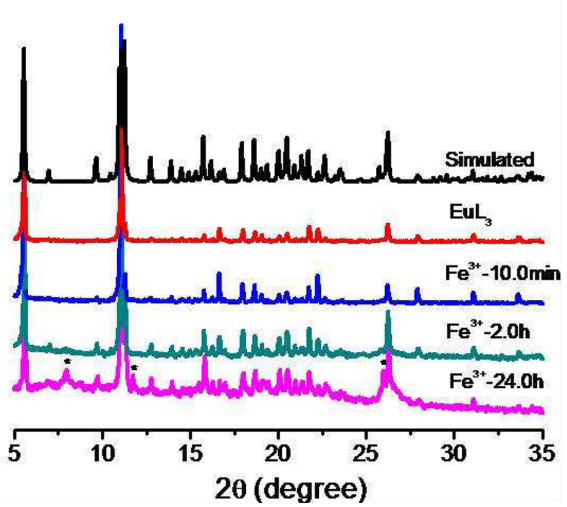

Figure 6. Powder XRD patterns of pristine **EuL_3** and **EuL_3** treated in 0.01 mol/L of Fe^{3+} solution for different times; the new peaks are marked with asterisks.

terpyridine groups, when the immersing time is 2 h, the PL intensity of the sample decreases to 6.3%. In case that all free terpyridine groups are coordinated, the Eu cations of **EuL_3** will be gradually exchanged by Fe^{3+} so that the PL is totally quenched when the sample is treated in Fe^{3+} solution for 24 h. This speculation is further confirmed by the TGA analyses of **EuL_3** and the Fe^{3+}-**EuL_3**, (Supporting Information Figure S1). It is observed that **EuL_3** has good thermal stability, it is stable up to 490 °C, and the final residue is composed of Eu_2O_3 (8.8%). The TGA result of Fe^{3+}-**EuL_3** (Fe^{3+}-24h) shows that the 11.1% weight loss before 320 °C corresponds to the removal of solvent molecules; 57.4% weight loss between 320 and 435 °C results from the loss of the organic component in the framework built of Fe^{3+} and terpyridine, while the weight loss of 16.2% between 435 and 535 °C is due to the loss of the organic component in the framework built of Eu^{3+} and terpyridine. The final residues are composed of Fe_2O_3 and Eu_2O_3 (15.4%).

In order to elucidate the possible mechanism for such photoluminescence quenching by the metal ions, powder XRD was employed to monitor the structure changes during Fe^{3+} solution treatment. The powder XRD patterns of the samples of **EuL_3** immersed in Fe^{3+} solution for 10 min and 2 h are similar to that of pristine **EuL_3** (Figure 6), suggesting that the main framework of **EuL_3** crystals does not change although the photoluminescence is mostly quenched. It can be concluded that the PL quenching within a short period mainly results from complex formation between the receptor unit (terpyridine) and analyte (Fe^{3+}). Twenty-four hours later, a few new peaks (marked with asterisks) come out in the XRD pattern besides the pattern of EuL_3. That indicates that a new kind of structure may form after a long time of immersing. However, the main framework of EuL_3 does not change.

It is well-known that a typical fluorescence probe contains a receptor unit, a luminescence center, and a linker. In the framework of **EuL_3**, Eu is the luminescence center, while the ligand **L** functions as both a linker and a receptor. On the one hand, one-third of the **L** ligands are located on the main chain, and they act as chemical linkers of adjacent Eu ions, with the carboxylate group connected to one Eu ion and the terpyridine moieties chelated to the other Eu ion to form a 1D infinite chain; on the other hand, two-thirds of the **L** ligands are perpendicular to the main chain, and they not only provide receptors for Fe^{3+} but also act as an optical linker between the central Eu ions and the Fe^{3+} ions. Once the Fe^{3+} ions in the solution are captured by the free terpyridine groups to form Fe-terpyridine complexes, the energy transfer process from **L** to the central Eu^{3+} ions will be forbidden, resulting in fluorescence quenching of **EuL_3**. (Scheme 1, Step 1). Furthermore, the

Scheme 1. Possible Mechanism of Fluorescence Quenching of EuL_3 by Fe^{3+}

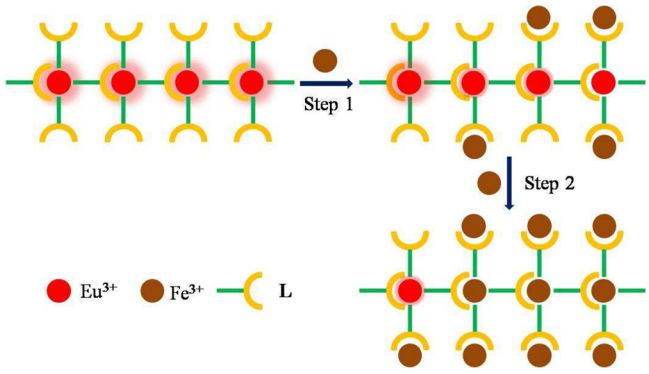

channels in **EuL_3** enable Fe^{3+} ions to pass through crystals smoothly, and therefore, the photoluminescence of **EuL_3** crystals can be quenched in a very short period. Finally, the Eu^{3+} ions in the **EuL_3** are replaced by Fe^{3+} ions for long time immersion, and some original frameworks rearrange to form new frameworks. However, the main framework of EuL_3 still keeps its original structure (Scheme 1, Step 2).

To explore the potential of such a highly selective and sensitive MOF sensor in a biological system, **EuL_3** was immersed in the simulated physiological conditions (0.02 mol/L HEPES aqueous buffer solution, pH = 7) with different concentrations of Fe^{3+} ions. The luminescence tests (Figure 7a) and XRD (Figure 7b) were then carried out on **EuL_3** crystals. With increasing concentration of Fe^{3+} ions, the luminescence intensity of Eu decreased dramatically. The Eu luminescence was almost completely quenched when the Fe^{3+}-concentration was increased to 0.01 mol/L. The PXRD results suggest that

dx.doi.org/10.1021/am302862k | ACS Appl. Mater. Interfaces 2013, 5, 1078−1083

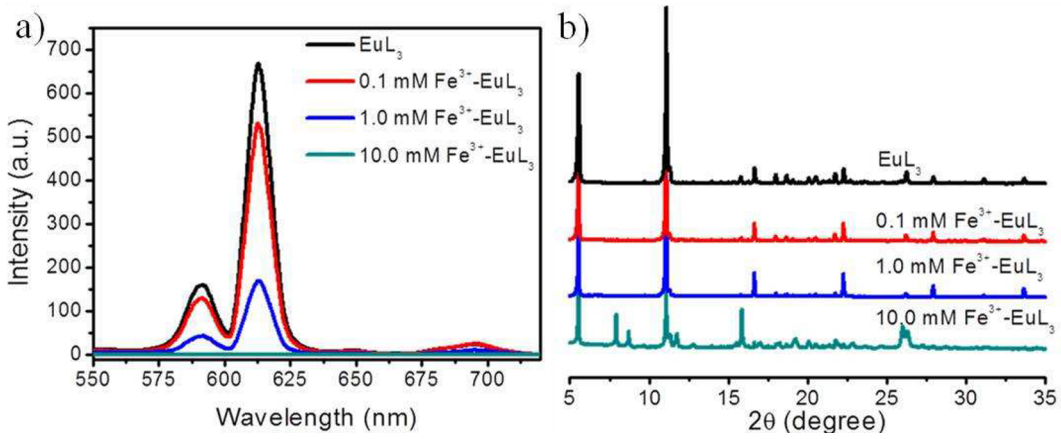

Figure 7. (a) Emission spectra and (b) powder XRD patterns of pristine $\mathbf{EuL_3}$ and $\mathbf{EuL_3}$ after immersing in HEPES aqueous buffer solution containing different concentrations of Fe^{3+} ions for 24 h.

the original frameworks of $\mathbf{EuL_3}$ transformed after immersion in HEPES/(0.01 mol/L Fe^{3+} ions) solution for 24 h. In conclusion, compound $\mathbf{EuL_3}$ displays fluorescence behavior under biological condition similar to that in aqueous solution, and therefore, it can be used as a promising luminescence sensor for Fe^{3+} ions in a biological system.

In order to make the detection simple and portable, we developed a fluorescence test paper for rapid detection of Fe^{3+} in aqueous solution. The test paper was prepared by immersing a filter paper (1×2.5 cm^2) in the dispersion of ground EuL_3 in ethanol and drying it at room temperature. For the detection of Fe^{3+} in water, the test paper was immersed $Fe(NO_3)_3$ aqueous solutions for 1 min and then exposed to air for drying. As shown in Figure 8, under the irradiation of UV light of 365 nm,

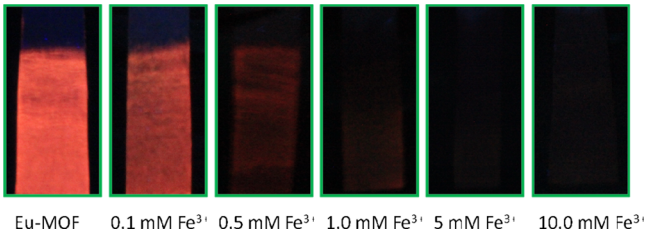

Figure 8. Optical images of the $\mathbf{EuL_3}$ test paper after immersion into solutions with different concentrations of $Fe(NO_3)_3$ for 1 min.

the test paper showed a bright red color. The fluorescent colors of the test paper changed to red, dark red, faint dark red, and finally black as soaked in 0.0001, 0.0005, 0.001, and 0.005 mol/L of $Fe(NO_3)_3$ aqueous solution. To the naked eye, one can distinguish the colors of different intensities.

CONCLUSIONS

We have demonstrated a highly selective and sensitive method to detect Fe^{3+} ions in aqueous solution or in biological systems based on the specific affinity between Fe^{3+} ions and chelating terpyridyl sites in $\mathbf{EuL_3}$. On the basis of the fluorescence quenching of $\mathbf{EuL_3}$ caused by Fe^{3+} ions, the Fe^{3+} ions of as low as 0.0005 mol/L can be detected without interference from other metallic ions. By using this compound, a test paper was prepared easily and its response to Fe^{3+} ions in one minute was visible to the naked eye. Therefore, $\mathbf{EuL_3}$ and its test paper may find practical applications in the laboratory and in daily life in the near future.

ASSOCIATED CONTENT

Supporting Information

Crystal data and TGA curve of $\mathbf{EuL_3}$. This material is available free of charge via the Internet at http://pubs.acs.org.

AUTHOR INFORMATION

Corresponding Author

*E-mail: xiez@ciac.jl.cn (Z.X.), sunzc@ciomp.ac.cn (Z.S.).

Author Contributions

The manuscript was written through contributions of all authors.

Notes

The authors declare no competing financial interest.

ACKNOWLEDGMENTS

The financial support from the National Natural Science Foundation of China (No. 21201159, 61176016), China Postdoctoral Science Foundation Grant (No. 2012M510892), Science and Technology Department of Jilin Province (No. 20121801), and Returnee startup fund of Jilin is gratefully acknowledged. Z.S. thanks the support of the "Hundred Talent Program" of CAS, and Innovation and Entrepreneurship Program of Jilin.

REFERENCES

(1) Andrews, N. C. *N. Engl. J. Med.* **1999**, *341*, 1986−1995.
(2) Haas, J. D.; Brownlie, T. *J. Nutr.* **2001**, *131*, 676S−690S.
(3) Alez, G. *Iron Overload: Haemosiderosis, Causes, Primary and Secondary Haemochromatosis, Treatment, and More*; Webster's Digital Services: 2012; pp 1−204.
(4) Tesfaldet, Z. O.; van Staden, J. F.; Stefan, R. I. *Talanta* **2004**, *64*, 1189−1195.
(5) Akatsuka, K.; McLaren, J. W.; Lam, J. W.; Berman, S. S. *J. Anal. At. Spectrom.* **1992**, *7*, 889−894.
(6) Elrod, V. A.; Johnson, K. S.; Coale, K. H. *Anal. Chem.* **1991**, *63*, 893−898.
(7) Ohashi, A.; Ito, H.; Kanai, C.; Imura, H.; Ohashi, K. *Talanta* **2005**, *65*, 525−530.
(8) Valeur, B.; Leray, I. *Coord. Chem. Rev.* **2000**, *205*, 3−40.
(9) Horcajada, P.; Gref, R.; Baati, T.; Allan, P. K.; Maurin, G.; Couvreur, P.; Férey, G.; Morris, R. E.; Serre, C. *Chem. Rev.* **2011**, *112*, 1232−1268.
(10) Cui, Y.; Yue, Y.; Qian, G.; Chen, B. *Chem. Rev.* **2011**, *112*, 1126−1162.

(11) Kreno, L. E.; Leong, K.; Farha, O. K.; Allendorf, M.; Van Duyne, R. P.; Hupp, J. T. *Chem. Rev.* **2011**, *112*, 1105−1125.
(12) Xu, H.; Liu, F.; Cui, Y.; Chen, B.; Qian, G. *Chem. Commun.* **2011**, *47*, 3153.
(13) Rieter, W. J.; Taylor, K. M. L.; Lin, W. *J. Am. Chem. Soc.* **2007**, *129*, 9852−9853.
(14) Chen, B.; Yang, Y.; Zapata, F.; Lin, G.; Qian, G.; Lobkovsky, E. B. *Adv. Mater.* **2007**, *19*, 1693−1696.
(15) Hanaoka, K.; Kikuchi, K.; Kojima, H.; Urano, Y.; Nagano, T. *Angew. Chem.* **2003**, *115*, 3104−3107.
(16) Chen, B.; Wang, L.; Zapata, F.; Qian, G.; Lobkovsky, E. B. *J. Am. Chem. Soc.* **2008**, *130*, 6718−6719.
(17) Cui, Y.; Xu, H.; Yue, Y.; Guo, Z.; Yu, J.; Chen, Z.; Gao, J.; Yang, Y.; Qian, G.; Chen, B. *J. Am. Chem. Soc.* **2012**, *134*, 3979−3982.
(18) Liu, W.; Jiao, T.; Li, Y.; Liu, Q.; Tan, M.; Wang, H.; Wang, L. *J. Am. Chem. Soc.* **2004**, *126*, 2280−2281.
(19) Chen, B.; Wang, L.; Xiao, Y.; Fronczek, F. R.; Xue, M.; Cui, Y.; Qian, G. *Angew. Chem., Int. Ed.* **2009**, *48*, 500−503.
(20) Xiao, Y.; Cui, Y.; Zheng, Q.; Xiang, S.; Qian, G.; Chen, B. *Chem. Commun.* **2010**, *46*, 5503−5505.
(21) Hu, R.; Feng, J.; Hu, D.; Wang, S.; Li, S.; Li, Y.; Yang, G. *Angew. Chem., Int. Ed.* **2010**, *49*, 4915−4918.
(22) Weerasinghe, A. J.; Schmiesing, C.; Varaganti, S.; Ramakrishna, G.; Sinn, E. *J. Phys. Chem. B* **2010**, *114*, 9413−9419.
(23) Weerasinghe, A. J.; Abebe, F. A.; Sinn, E. *Tetrahedron Lett.* **2011**, *52*, 5648−5651.
(24) Dang, S.; Ma, E.; Sun, Z.-M.; Zhang, H. *J. Mater. Chem.* **2012**, *22*, 16920−16926.
(25) Formica, M.; Fusi, V.; Giorgi, L.; Micheloni, M. *Coord. Chem. Rev.* **2012**, *256*, 170−192.
(26) Sahoo, S. K.; Sharma, D.; Bera, R. K.; Crisponi, G.; Callan, J. F. *Chem. Soc. Rev.* **2012**, *41*, 7195−7227.
(27) Jia, J.; Lin, X.; Blake, A. J.; Champness, N. R.; Hubberstey, P.; Shao, L.; Walker, G.; Wilson, C.; Schröder, M. *Inorg. Chem.* **2006**, *45*, 8838−8840.
(28) Constable, E. C.; Dunphy, E. L.; Housecroft, C. E.; Neuburger, M.; Schaffner, S.; Schaper, F.; Batten, S. R. *Dalton Trans.* **2007**, 4323−4332.
(29) Wu, Q.-R.; Wang, J.-J.; Hu, H.-M.; Shangguan, Y.-Q.; Fu, F.; Yang, M.-L.; Dong, F.-X.; Xue, G.-L. *Inorg. Chem. Commun.* **2011**, *14*, 484−488.